Sediment management modelling in the Blue Nile Basin using SWAT model

Getnet D. Betrie[1,2], Yasir. A. Mohamed[1,2], A. van Griensven[1], Raghavan Srinivasan[4], and A. Mynett [1,2,3]

[1]UNESCO-IHE Institute for Water Education, P.O.Box 3015, 2601DA Delft, The Netherlands

[2] Delft University of Technology, PO Box 5048, 2600 GA Delft, The Netherlands.

[3]Deltares-Delft Hydraulics, PO Box 177, 2600 MH Delft, The Netherlands

[4]Texas A&M University, College Station, Texas, USA

Correspondence to: G.D. Betrie (g.betrie@unesco-ihe.org)

Abstract

Soil erosion/sedimentation is an immense problem that has threatened water resources development in the Nile, particularly in Eastern Nile (Ethiopia, Sudan and Egypt). An insight into soil erosion/sedimentation mechanism and mitigation methods plays an imperative role for the sustainable water resources development in the region. This paper presents daily sediment yield simulation in the Upper Blue Nile under different Best Management Practices (BMPs) scenarios. Scenarios were existing condition, filter strips, stone bunds (parallel terrace), and reforestation. The Soil and Water Assessment Tool (SWAT) was used to model soil erosion, identify soil erosion prone areas and assess the impact of BMPs on sediment reduction. The study found satisfactory agreement between daily observed and simulated sediment concentrations with Nash-Sutcliffe efficiency (NSE) = 0.88, percent bias (PBIAS) = -0.05%, and ratio of the root mean square error to the standard deviation of measured data (RSR) = 0.35 for calibration and NSE = 0.83, RSR = 0.61 and PBIAS = -11 % for validation. The sediment yield for baseline scenario was 117×10^6 tyr^{-1}. The filter strips, stone bunds and reforestation reduced the sediment yield at the outlet of the Upper Blue Nile basin by 44%, 41% and 11%, respectively. The sediment reduction at subbasins outlets varied from 29% to 68% by filter strips, 9% to 69% by stone bunds and 46% to 77% by reforestation. This study indicates that BMPs are very useful in reducing sediment transport and could be used for reservoirs sedimentation management in the Eastern Nile basin.

1 Introduction

The Blue Nile River, which originates from the steep mountains of the Ethiopian Plateau, is the major source of sediment load in the Nile basin. Soil erosion upstream and the subsequent downstream sedimentation has been an immense problem threatening the existing and future water resources development in the Nile basin. The benefits gained by construction of micro-dams in the Upper Nile, have been threatened by the rapid loss of storage volume due to excessive sedimentation (El-Swaify and Hurni, 1996; Tamene et al. 2006). Moreover, the green water storage of the Ethiopian highlands, where rainfed agriculture prevails has been diminished because of top-soil loss and this has caused frequent agricultural drought (Hurni, 1993; El-Swaify and Hurni, 1996). On the downstream part of the basin (e.g., in Sudan and Egypt) excessive sediment load has demanded for massive operation cost of irrigation canals desilting, and sediment dredging in front of hydropower turbines. For example, the Sinnar dam has lost 65% of its original storage after 62 yr operation (Shahin, 1993) and the other dams (e.g., Rosieres and Khashm el Girba) lost similar proportions since construction (Ahmed, 2004). Both the Nile Basin Initiative and the Ethiopian government are developing ambitious plans of water resources projects in the Upper Blue Nile basin, locally called the Abbay basin (BCEOM, 1998; World Bank, 2006). Thus, an insight into the soil erosion/sedimentation mechanism and the mitigation measures plays an indispensable role for the sustainable water resources development in the region.

Literature shows several catchment models that are proven to understand the soil erosion/sedimentation processes and mitigation measures (Merritt et al., 2003; Borah and Bera, 2003). Nevertheless, there are a few applications of erosion modelling in the Upper Blue Nile basin. These include Zeleke (2000), Haregeweyn and Yohannes (2003), Mohamed et al. (2004), Hengsdijk et al. (2005), Steenhuis et al., (2009), and Setegn et al. (2010). Zeleke (2000) simulated soil loss using the Water Erosion Prediction Project (WEPP) model and the result slightly underestimated the observed soil loss in the Dembecha catchment (27,100 ha). Haregeweyn and Yohannes (2003) applied the Agricultural Non-Point Source (AGNPS) model and well predicted sediment yield in the Augucho catchment (224 ha). The same AGNPS model was used by Mohamed et al (2004) to simulate sediment yield in the Kori (108 ha) catchment and the result was satisfactory. Hengsdijk et al. (2005) applied the Limburg Soil Erosion Model (LISEM) to simulate the effect of reforestation on soil erosion in the Kushet – Gobo Deguat

catchment (369 ha), but the result raised controversy by Nyssen et al. (2005). The SWAT model was applied for simulation of a sediment yield by Setegn et al. (2010) in the Anjeni gauged catchment (110 ha) and the obtained result was quite acceptable. Steenhuis et al. (2009) calibrated and validated a simple soil erosion model in the Abbay (Upper Blue Nile) basin and reasonable agreement was obtained between model predictions and the 10-day observed sediment concentration at El Diem located at the Ethiopia-Sudan border.

Most of the above applications are successfully attempted to estimate sediment yield at small catchment scale or evaluate soil erosion model. Yet literature shows a lack of information on mitigation measures in the upper Blue Nile basin. Therefore, the objective of this study is to model the spatially distributed soil erosion/sedimentation process over the Upper Blue Nile basin at a daily time step and assess the impact of different catchment management interventions on soil erosion and ultimately on sediment yield.

A brief description of the Upper Blue Nile Basin is given in the next section, followed by discussion of the methodology used. The third section presents the model results and discussion of different land management scenarios. Finally, the conclusion summarizes the main findings of the investigation.

2 Description of study area

The Upper Blue Nile River basin has a total area of 184, 560 km^2, and is shown in Fig. 1. The Ethiopian Plateau has been deeply incised by the Blue Nile River and its tributaries, with a general slope to the northwest. The elevation ranges from 500 m at Sudan border to 4230 m at the top of highlands. The Didessa and Dabus tributaries, draining the south-western part of the basin contribute about one third of the total flow. The climate over the Blue Nile is governed by the seasonal migration of the Inter Tropical Convergence Zone ITCZ from south to north and back. The annual rainfall varies from 900 mm near the Ethiopia/Sudan boarder to 2200 mm over Didessa and Dabus. Since the rainfall is highly seasonal, the Blue Nile possesses a highly seasonal flood regime with over 80% of annual discharge (~ 50 billion m^3) occurring in the four months from July to October, while 4% of the flow occurs during the driest period from January to April (Sutcliffe and Parks, 1999). In the basin the minimum and maximum temperatures are 11 ^{0}c and 18 ^{0}c, respectively. The dominant soil types are Alisols and Leptosols 21%, followed by Nitosoils 16%, Vertisols 15% and Cambisols 9%.

3 Methodology

3.1 SWAT model description

The Soil and Water Assessment Tool (SWAT) is a physical process based model to simulate continuous-time landscape processes at catchment scale (Arnold et al., 1998; Neitsch et al., 2005). The catchment is divided into hydrological response units (HRU) based on soil type, land use and slope classes. The hydrology computation based on daily precipitation, runoff, evapotranspiration, percolation and return flow is performed at each HRU. The SWAT model has two options for computing surface runoff: (i) the Natural Resources Conservation Service Curve Number (CN) method (USDA-SCS, 1972) or (ii) the Green and Ampt method (Green and Ampt, 1911). Similarly, there are two options available to compute peak runoff rate: (i) the modified rational formula (Kuichling, 1989) or (ii) the SCS TR-55 method (USDA-SCS, 1986). The flow routing in the river channels is computed using the variable storage coefficient method (Williams, 1969), or Muskingum method (Chow, 1959). SWAT includes three methods for estimating potential evapotranspiration: (i) Priestley-Taylor (Priestley and Taylor, 1972), (ii) Penman-Monteith (Monteith, 1965) and (iii) Hargreaves (Hargreaves and Riley, 1985).

SWAT employs the Modified Universal Soil Loss Equations (MUSLE) to compute HRU-level soil erosion. It uses runoff energy to detach and transport sediment (Williams and Berndt, 1977). The sediment routing in the channel (Arnold et al, 1995) consists of channel degradation using stream power (Williams, 1980) and deposition in channel using fall velocity. Channel degradation is adjusted using USLE soil erodibility and channel cover factors.

3.2 SWAT model setup

The SWAT model inputs are Digital Elevation Model (DEM), landuse map, soil map, and weather data, which is shown in Table 1. The ArcGIS interface (Winchell et al., 2007) for the SWAT2005 version was used to extract the SWAT model input files. The DEM was used to delineate the catchment and provide topographic parameters such as overland slope and slope length for each subbasin. The catchment area of the Upper Blue Nile was delineated and discretized into 15 subbasins using a 90 m DEM (http://srtm.csi.cgiar.org).

The landuse map of the Global Land Cover Characterization (GLCC) was used to estimate vegetation and their parameters input to the model. The GLCC is part of the United States Geological Survey (USGS) database, with a spatial resolution of 1 km and 24 classes of landuse

representation (http://edcsns17.cr.usgs.gov/glcc/glcc.html). The parameterization of the landuse classes (e.g. leaf area index, maximum stomatal conductance, maximum root depth, optimal and minimum temperature for plant growth) is based on the available SWAT landuse classes. Table 2 shows the land use and land cover types and their area coverage in the Upper Blue Nile. The land cover classes derived are Residential area 0.2%, Dryland Cropland 17%, Cropland 5.8%, Grassland 2.5%, Shrubland 1.1%, Savanna 68.8%, Deciduous Forest 0.02%, Evergreen Forest 1.6%, Mixed Forest 0.7%, Water Body 2.2%, and Barren 0.4%.

The soil types for the study area were extracted from the SOIL-FAO database, Food and Agriculture Organization of the United Nations (FAO, 1995). There are around 23 soil types, at a spatial resolution of 10 km with soil properties for two layers (0-30 cm and 30-100 cm depth). The soil properties (e.g. particle-size distribution, bulk density, organic carbon content, available water capacity, and saturated hydraulic conductivity) were obtained from Batjes (2002).

The USGS landuse, the FAO soil and the slope class maps were overlaid to derive 1747 unique HRUs. Although the SWAT model provides an option to reduce the number of HRUs in order to decrease the computation time required for the simulation, we considered all of the HRUs to evaluate the watershed management intervention impact.

The daily precipitation and maximum and minimum temperature data at 17 stations interpolated spatially over the catchments were used to run the model. Most of the stations were either established recently or had a lot of missing data. Therefore, a weather generator based on monthly statistics was used to fill in the gaps. Solar radiation and wind speed were generated by the weather generator.

Daily river flow and sediment concentration data measured at El Diem gauging station (see Fig. 1) were used for model calibration and validation. The flow observations were available throughout the year, while the sediment concentration was usually monitored during the main rainy season, June to October. The Blue Nile water is relatively sediment free during the remaining months.

The model was run daily for 12 years; the period from 1990 to 1996 was used for calibration whereas the period from 1998 to 2003 was used for validation. The modelling period selection considered data availability and avoided rapid landuse/ cover change that was documented as alarming until the late 1980's by Zeleke et al. (2000) and Zeleke and Hurni (2001). Daily flow and sediment discharge were used to calibrate and validate the model at El Diem gauging station,

located at the Ethiopia-Sudan border. Although we know that calibrating the model at subbasins outlet would improve the spatial parameter distribution, we could not perform it due to lack of data. Sensitivity analysis was carried out to identify the most sensitive parameters for model calibration using One-factor-At-a-Time (LH-OAT), an automatic sensitivity analysis tool implemented in SWAT (van Griensven et al., 2006). Those sensitive parameters were automatically calibrated using the Sequential Uncertainty Fitting (SUFI-2) algorithm (Abbaspour et al., 2004; Abbaspour et al., 2007).

3.3 Model performance evaluation

Model evaluation is an essential measure to attest the robustness of the model. In this study three model evaluation methods - (i) Nash-Sutcliffe efficiency (NSE), (ii) percent bias (PBIAS), and (iii) ratio of the root mean square error to the standard deviation of measured data (RSR) - were employed following Moriasi et al. (2007) model evaluation guidelines. The Nash-Sutcliffe efficiency (NSE) is computed as the ratio of residual variance to measured data variances (Nash and Sutcliffe, 1970), see Eqs. (1).

$$NSE = 1 - \left[\frac{\sum_{i}^{n} \left(X_i^{obs} - X_i^{sim} \right)^2}{\sum_{i}^{n} \left(X_i^{obs} - X^{mean} \right)^2} \right] \quad (1)$$

Where:

X_i^{obs} = observed variable (flow in m^3/s or sediment concentration in mg/l).
X_i^{sim} = simulated variable (flow in m^3/s or sediment concentration in mg/l).
X^{mean} = mean of n values.
n = number of observations.

~~The NSE value ranges between $-\infty$ and 1; a value between 0 and 1 indicates acceptable model performance whereas values $\leq$ 0 indicates the mean observed values is better than the simulated values and hence, indicates unacceptable performance (Nash and Sutcliffe, 1970).~~

The Percent bias (PBIAS) measures the average tendency of the simulated data to be larger or smaller than their observed counterparts (Gupta et al., 1999), see Eqs. (2).

$$PBIAS = \left[\frac{\sum_{i}^{n} \left(X_i^{obs} - X_i^{sim} \right) \times 100}{\sum_{i}^{n} \left(X_i^{obs} \right)} \right] \quad (2)$$

~~The optimal value of PBIAS is 0, with low-magnitude values indicating accurate model simulation. Positive values indicate model underestimation bias, and negative values indicate model overestimation bias (Gupta et al., 1999).~~

The ratio of root mean square error to the standard deviation of measured data (RSR) is calculated as the ratio of the Root Mean Square Error (RMSE) and standard deviation of the observed data (Moriasi et al., 2007), see Eqs. (3):

$$RSR = \frac{RMSE}{STDEV_{obs}} = \left[\frac{\sqrt{\sum_{i}^{n} \left(X_i^{obs} - X_i^{sim} \right)^2}}{\sqrt{\sum_{i}^{n} \left(X_i^{obs} - X^{mean} \right)^2}} \right] \quad (3)$$

~~RSR varies from zero (optimal) to a large positive value. The lower RSR, the lower is the RMSE, and hence better the model performance (Moriasi, et al., 2007).~~

According to Moriasi, et al. (2007) simulation judged as satisfactory if NSE > 0.5, RSR ≤ 0.70 and PBIAS= ± 25% for flow and NSE > 0.5, RSR ≤ 0.70 and PBIAS= ± 55% for sediment.

3.4 Catchment management intervention scenarios

Catchment management intervention involves an introduction of best management practices (BMPs) to reduce soil erosion and sediment transport. The SWAT model was applied to simulate the impact of BMPs on sediment reduction in the USA (Vache et al., 2002; Santhi et al., 2005; Bracmort et al., 2006). The BMPs were represented in the SWAT model by modifying SWAT parameters to reflect the effect the practice has on the processes simulated (Bracmort et al., 2006). However, the type of BMPs and their parameter value selection is site specific and ought to reflect the study area reality. Thus, we cautiously selected appropriate BMPs and their parameter value based on documented local research experience in the Ethiopian highlands (Hurni, 1985; Herweg and Ludi, 1999; Gebremichael et al., 2005). The three selected BMPs were (i) filter strips, (ii) stone bunds (parallel terrace locally built from stone along the contour), and (iii) reforestation. Each BMP has a different effect on flow and sediment variables and is represented by distinct parameter(s) in the SWAT model. Table 3 shows the SWAT parameters

used to represent BMPs. The parameter used to simulate the effect of filter strip is width of filter strip (FILTERW). The effect of stone bund was simulated using Curve Number (CN2), average slope length (SLSUBBSN) and USLE support practice factor (USLE_P). The reforestation effect was simulated by introducing land use change.

A total of four model scenarios were run as depicted in Table 3. In Scenario-0, the basin existing condition was considered. In Scenario-1, filter strips were placed on all agricultural HRUs that are a combination of dryland cropland, all soil types and slope classes. The effect of the filter strip is that it filters the runoff and traps the sediment in a given plot (Bracmort et al., 2006). We simulated the impact of filter strips on sediment trapping by assigning FILTERW value of 1m. The FILTERW value was modified by editing the HRU (.hru) input table. This filter width value was assigned based on local research experience in the Ethiopian highlands (Hurni, 1985; Herweg and Ludi, 1999).

In Scenario-2, stone bunds were placed on agricultural HRUs that are a combination of dryland cropland, all soil types and slope classes. This practice has a function to reduce overland flow, sheet erosion and reduce slope length (Bracmort et al., 2006). We modified SLSSUBSN value by editing the HRU (.hru) input table, whereas USLE_P and CN2 values were modified by editing Management (.mgt) input table using the SWAT model interface. The SWAT model assigns the SLSUBBSN parameter value based on the slope classes. In this application the assigned values by the SWAT were 61 m, 24 m and 9.1 m for slope class 0-10%, 10-20% and greater than 20%, respectively. The modified parameters values were SLSUBBSN is equal to 10 m for slope class 0-10% and 10-20% classes, USLE_P is equal to 0.32, and CN2 is equal to 59 as is depicted in Table 3. The SLSUBBSN represents the spacing between successive stone bunds at field condition and the modified value was used as reported by Hurni (1985) and Herweg and Ludi (1999). Similarly, USLE_P value was obtained from documented field experience by Gebremichael et al. (2005). The CN2 value was obtained from the SWAT user's manual version 2005 for contoured and terraced condition (Neitsch et al, 2005).

In Scenario-3, we simulated the impact of reforestation on sheet erosion. The reforestation has a function to reduce overland flow and rainfall erosivity. It was deemed impractical to change agricultural land into forest completely. Thus we replaced 8% of the area occupied by cropland, shrubland, barren, mixed forest, and deciduous forest into evergreen forest. The evergreen forest was selected since it has a wider coverage area than other types of forest in the study area, see

Table 2. The associated parameters (e.g., plant, hydrological and erosion) for the new landuse were changed by the SWAT model from the database. The parameters used to simulate the effect of reforestation on soil erosion were USLE cover factor (USLE_C) and curve number (CN2) and their values were assigned by SWAT model.

4 Results and discussion

The SWAT sensitive parameters and their calibrated values are shown in Table 4. Fourteen parameters were sensitive for flow simulation and eleven parameters were sensitive for sediment simulation. For brevity, three flow and four sediment sensitive parameters are discussed below. The three sensitive parameters for flow are curve number (CN2), baseflow alpha factor (ALPHA_BF), and recharge to deep aquifer fractions (RCHRG_DP). The fitted parameter value for CN2 was adjusted multiplying the typical value from the SWAT database by one plus -0.02. While the fitted value for ALPHA_BF, and RCHRG_DP were 0.29 and 1.07, respectively. The four sensitive parameters for sediment were linear re-entrainment parameter for channel sediment routing (SPCON), USLE cover factor (USLE_C), exponent of re-entrainment parameter for channel (SPEXP) and channel erodibility factor, (Ch_Erod). The fitted value for USLE_C cover factor varies for different land cover and the assigned values were USLE_C{Dryland-crop}=0.29, USLE_C{Cropland}=0.03, USLE_C{Savanna}=0.17, USLE_C{Grassland}=0.35, and USLE_C{Shurbland}=0.36. The calibrated values for SPCON, SPEXP, Ch_Erod were 0.01, 1.20 and 0.63, respectively.

The SWAT hydrology predictions were calibrated against daily flow from 1990 to 1996 and validated from 1998 to 2003 at El Diem gauging station (Ethiopia-Sudan border). The model flow predictions fitted the observed flow well as showed by acceptable values of the NSE, RSR and PBIAS. The simulated daily flow matched the observed values for calibration period with NSE, RSR and PBIAS is equal to 0.68, 0.57, and 10%, respectively. For the validation period, the simulated daily flow matched the observed values with NES, RSR and PBIAS equal to 0.63, 0.61 and -8 %, respectively. Aggregated daily flow values into monthly average improved the model results. The monthly flow simulation matched the observed for calibration period with NES=0.82, RSR=0.42 and PBIAS=10% and NES= 0.79, RSR= 0.46, and PBIAS= -8% for validation. ~~According to Moriasi, et al. (2007) flow simulation judged as satisfactory if NSE >~~

~~0.5, RSR ≤ 0.70 and PBIAS= ± 25%. Thus we found the model performance quite satisfactory both for calibration and validation periods.~~

A comparison between observed and simulated daily flow for the calibration and validation periods is depicted in Fig. 2. The year 2001 is not presented in validation period since the observed data is missing. The model slightly overestimated rising limb and slightly underestimated recession limb in calibration and validation periods. This could be due to the maximum soil depth (≤ 100 cm) that was obtained from the FAO data does not well represent the soil depth distribution of the basin. In fact, literature shows that the soil depth of the basin is very deep (>150 cm) in the south-west, moderately deep (100-150 cm) in the central, and shallow (30-50 cm) in the north-east and east (FAO, 1986; BCEOM, 1999). Thus, the model did not abstract the right amount of precipitation before surface runoff generation. Subsequently, the simulation was overestimated for the rising limb. This in turns caused less water storage in a shallow aquifer and underestimated the base-flow for the receding limb. The model simulated the peak flow during the calibration periods except in the year 1994. However, the model slightly overestimated the peak flow in the validation period. There could be various reasons for the peak mismatch but it is most likely attributed to precipitation data since it had a lot of missing data. Literature has also reported that precipitation data is the main constraint for accurate modelling of discharge in the Blue Nile (Steenhuis et al., 2009). It is interesting that the model well captured the rising and the falling limbs of the wet-season flow which is very important for sediment simulation, which is shown in Fig. 3.

The SWAT sediment predictions were calibrated against measured data from 1990 to1996 and validated from 1998 to 2003 at El Diem gauging station using daily sediment concentrations. However, sediment concentrations data are available only for the rainy season, which occurs from July to October. ~~The calibration and validation periods model performance for the daily sediment simulation is shown in Table 5.~~ The model sediment predictions fitted the observed concentrations very well as indicated by acceptable values of the NSE, RSR and PBIAS. The simulated daily sediment concentrations matched the observed concentrations for calibration period with NSE, RSR and PBIAS is equal to 0.88, 0.35, and -0.05%, respectively. The daily simulated sediment concentrations for the validation period showed agreement with the observed concentrations with NES, RSR and PBIAS equal to 0.83, 0.61 and -11 %, respectively. Aggregating daily sediment concentrations into monthly average improved the model

predictions. The simulated monthly sediment concentrations matched the observed sediment concentrations with NES= 0.92, RSR= 0.29, and PBIAS= -0.21% for calibration and NES= 0.88, RSR= 0.34, and PBIAS= -11% for validation. Furthermore, we found our model performance comparable to the recent results reported by Steenhuis et al. (2009). Their results stated that NSE = 0.75 for the calibration and NSE=0.69 for the validation at El Diem gauging station.

The comparison between observed and simulated daily sediment concentrations for the calibration and validation periods is shown in Fig. 4. The model well simulated sediment concentrations on the rising and the falling limbs of the sediment hydrograph during the calibration period. Although the sediment peak was well captured in most of the years, the model slightly underestimated the peaks in 1993 and 1994. In contrast, the validation period overestimated peak concentration except in 1998. The model well simulated the rising limb sediment concentrations for the whole validation period. On the falling limb, however, the model well simulated the sediment concentrations except in 2002 and 2003.

Assessment of spatial variability of soil erosion is useful for catchment management planning. Fig. 5 shows the relative soil erosion prone areas in the Upper Blue Nile basin. The SWAT model simulation shows the soil erosion extent varies from negligible erosion to more than 150 t/ha. The soil erosion in the basin classified into low (0-20 t/ha/yr), moderate (20-70 t/ha/yr), severe (70-150 t/ha/yr) and extreme (≥ 150 t/ha/yr) categories. The low-class represents the erosion extent less than the soil formation rates, which is 22 t/ha/yr in the Ethiopian highlands (Hurni, 1983). The moderate-class represents erosion level less than the average soil loss from cultivated land, which is 72 t/ha/yr (Hurni, 1985). The extreme-class represents one fold higher than the average soil loss and the severe-class represents two folds higher than average soil loss. The extreme erosion was observed in the cultivated land and low erosion was observed in the savannah land. Subbasins 2, 3, and 4 were dominated by extreme soil erosion. Severe erosion was dominant in subbasins 8, 9, 12, 13 and 15. Moderate erosion was dominant in subbasins 1, 5, and 6; and low erosion was dominant in subbasins 7, 10, 11, and 14. These results indicate the erosion variations within a subbasin and the basin that is helpful to prioritise BMPs implementation area. Moreover, results showed that the sediment transport to the main river decreases from the north-east to south-west of the basin. However, emphasis should be given to relative erosion level than the absolute values because the model was not parameterized at outlets of subbasins due to lack of data.

The observed average sediment yield at the outlet of the Upper Blue Nile was 131 × 10^6 tyr^{-1}. The SWAT model predicted 117×10^6 tyr^{-1} for the existing condition. This result is quite comparable to 140×10^6 tyr^{-1} estimate by NBCBN (2005) that includes bed load as well. The bed load approximately accounts for 25% of the total load. However, running the model with different catchment management scenarios provided very interesting results. The implementations of filter strips have reduced the total sediment yield to 66×10^6 tyr^{-1} at El Diem, equivalent to 44% reduction. The stone bunds have reduced the total sediment yield to 70×10^6 tyr^{-1}, equivalent to 41% reduction. The reforestation has given the least reduction of sediment load (104×10^6 tyr^{-1}) at El Diem that is 11% reduction. The least sediment reduction by reforestation attributed to smaller implementation area (8% of the total basin area) unlike the two BMPs, which were implemented at 17% of the total basin area as is depicted in Fig. 6. In addition, the effect of reforestation on sediment reduction is masked by higher sediment yield from the agricultural land. The filter strips showed higher sediment reductions than stone bunds for the equal implementation area. ~~We found the BMPs efficiency rate on sediment reduction quite within the range as documented in literature (e.g., Vache et al., 2002).~~

The impact of BMPs at subbasins scale showed a wider spatial variability on sediment reduction as is shown in Fig. 7. The sediment reduction varied from 29% to 68% by filter strips, 9% to 69% by stone bunds and 46% to 77% by reforestation. The least reduction for filter strips (29%) and stone bunds (10% and 9%) were exhibited by subbasins 3 and 8. Conversely, the reforestation has reduced the sediment yield by 46% in subbasin 3 and 8. It was observed that filter strips and stone bunds effectiveness became greater as the agricultural area decrease and the proportion of the area for slope class ≤ 20% increase. This is expected because a higher overland flow concentration occurs as the steepness and a field size increase. The reforestation effectiveness became greater as the percent of agricultural area decrease in a subbasin. This was expected because the sediment yield from agricultural area is higher, and subsequently, masks the effectiveness of the reforestation on sediment reduction.

A comparison of percent of land placed in BMP and their effectiveness for each subbasin is depicted Table 5. Filter strips and stone bunds effectiveness were the highest in subbasins 4, 1 and 5, higher in subbasins 6, 11, 13, 10, 12 and 14, and low in the rest of subbasins. Reforestation effectiveness was the highest in subbasins 4, 1 and 14, higher in subbasins 9, 13, 5, 7, 5, 15 and 2 and low in the remaining subbasins. It is interesting that the highest reduction per

hectare was seen in the subbasins near the outlet. In general, the effectiveness of filter strips and stone bunds are consistent except subbasins 3 and 8, which are characterized by the steepest slope class. The effectiveness of reforestation is consistent in sediment reduction for the entire subbasins.

It is important to note that the reforestation effect is higher at the subbasin level than at the basin level. The reason is that the reforestation implementation area was proportional to filter strips and stone bunds at the subbasin level. For instance, in the subbasin-1, agricultural land covers 1.7% and reforestation covers 1% of the total area. In the basin level, however, the reforestation covers 8% and agricultural land cover 17% of the basin area, see Fig. 6. Thus, the effect of reforestation in the basin level was masked by the higher sediment yield from agricultural land. These results corroborate Santhi et al. (2005) findings that showed reductions in sediment and nutrient up to 99% at farm level and 1-2% at the watershed level.

Comparison of BMPs sediment reductions to literature in the Ethiopian highlands showed that results were reasonable. Filter strips sediment reductions were comparable to results reported by Herweg and Ludi (1999). These researchers reported 55%-84% of sediment yield reductions by filter strips on plot scale in the Ethiopian and Eritrean highlands. However, filter strips become less effective as the scale increase from plot to field due to flow concentration (Dillaha et al., 1989; Verstraeten et al., 2006). For instance, Verstraeten et al. (2006) reported low (20%) performance of filter strips due to overland flow convergence and sediment bypasses of filter-strips through ditches, sewers and culverts. However, we expect less overland flow convergence in the Blue Nile since the average farm size is less than ½ ha and the basin is unmanaged (e.g., residential area is <1%). Thus, the low scaling effect observed in this study could be attributed to this phenomenon. Stone bunds sediment yield reductions were quite comparable to results reported in literature (Herweg and Ludi, 1999; Gebremichael et al. 2005). Herweg and Ludi (1999) reported 72%-100% sediment yield reductions by stone bunds at plot scale in the Ethiopian and Eritrean highlands. Gebremichael et al. (2005) reported 68% of sediment yield reductions by stone bunds at field scale in the northern Ethiopia. It is worth noting that the scaling effect between plot and field is minimal even at field observation. The reforestation sediment yield reductions well agrees with Descheemaeker et al. (2005) that showed the complete sediment yield reductions by reforestation of degraded land in northern Ethiopia. The

higher sediment yield reductions observed by Descheemaeker et al. (2005) was due to the reforestation areas were located down-slope from cultivated land.

5 Conclusions

The SWAT model was applied to model spatially distributed soil erosion/sedimentation process at a daily time step and to assess the impact of three BMPs on sediment reduction in the Upper Blue Nile River basin. The model showed the relative erosion prone area that is helpful for catchment management planning. The total sediment yield for the existing condition at the basin outlet was 117×10^6 tyr^{-1}. Implementation of filter strips, stone bunds and reforestation have reduced the sediment yield at the outlet of the Upper Blue Nile by 44%, 41% and 11%, respectively. The reduction of sediment yield at 15 subbasins outlets varied from 29% to 68% by filter strips, 9% to 69% by stone bunds and 46% to 77% by reforestation. These results showed filter strips, stone bunds and reforestation are quite useful to reduce sediment yield in subbasins and the basin scales. However, their relative effectiveness are dependent upon the percent of land allocated, percent of slope class and implementation location in subbasins and the basin. Furthermore, the maximum benefit could be obtained by implementing the reforestation at a steep areas and others two BMPs at a low slope areas of the catchment.

The model results indicate that BMPs are very useful in reducing sediment transport and could be used for reservoirs sedimentation management in the Eastern Nile basin. An implementation of catchment management measures to reduce sediment yield involves use of resources. This type of research is very helpful for decision makers to evaluate the cost and benefits of BMP implementation. Nevertheless, the quantitative results may have some limitation because BMPs deterioration and gully erosion are not adequately represented in the SWAT model. Thus, more emphasis should be given to the relative estimates of the erosion than the magnitude.

Acknowledgements. The authors thank the EnviroGRIDS@BlackSea project under FP7 call FP7-ENV-2008-1, grant agreement No. 226740 for financial support of this research.

References

Abbaspour, K., Johnson, C., and van Genuchten, M.: Estimating uncertain flow and transport parameters using a sequential uncertainty fitting procedure, Vadose Zone J., 3, 1340-1352, 2004.

Abbaspour, K., Yang, J., Maximov, I., Siber, R., Bogner, K., Mieleitner, J., Zobrist, J., and Srinivasan, R.: Modelling hydrology and water quality in the pre-alpine/alpine Thur watershed using SWAT, J. Hydrol. , 333, 413-430, 2007.

Ahmed , A. A.: Sediment transport and watershed management component, Friend / Nile Project, Khartoum, 2004.

Arnold, J. G., Srinivasan, R., Muttiah, R. S., and Williams, J. R.: Large area hydrologic modeling and assessment part I: model development J. Am. Water Resour. As., 34, 73-89, 1998.

Arnold, J. G., Williams, J. R., and Maidment, D. R.: Continuous-time water and sediment-routing model for large basins, J. Hydraul. Eng-ASCE, 121, 171-183, 1995.

Batjes, N.: Revised soil parameter estimates for the soil types of the world, Soil Use Manage., 18, 232-235, 2002.

BCEOM: Abay River Basin integrated master plan, main report, Ministry of Water Resources, Addis Ababa, 1999.

Borah, D. K., and Bera, M.: Watershed-scale hydrologic and nonpoint-source pollution models: Review of mathematical bases, T. ASAE, 46, 1553-1566, 2003.

Bracmort, K., Arabi, M., Frankenberger, J., Engel, B., and Arnold, J.: Modeling long-term water quality impact of structural BMPs, T. ASABE, 49, 367-374, 2006.

Chow, V.T.: Open channel hydraulics, McGraw-Hill Book Company, New York, 1959.

Descheemaeker, K., Nyssen, J., Rossi, J., Poesen, J., Haile, M., Raes, D., Muys, B., Moeyersons, J., and Deckers, S.: Sediment deposition and pedogenesis in exclosures in the Tigray Highlands, Ethiopia, GEODERMA, 132, 291-314, 2006.

Dillaha, T., Reneau, R., Mostaghimi, S., and Lee, D.: Vegetative filter strips for agricultural nonpoint source pollution control, T. ASAE, 32, 513–519, 1989.

El-Swaify, S., and Hurni, H.: Transboundary effects of soil erosion and conservation in the Nile basin, Land Husbandry, 1, 6-21, 1996.

FAO: The Ethiopian highlands reclamation study (EHRS), Food and Agriculture Organization of the United Nations, Rome, 1986.

FAO: Digital Soil Map of the World and Derived Soil Properties, Food and Agriculture Organization of the United Nations, Rome, 1995.

Gebremichael, D., Nyssen, J., Poesen, J., Deckers, J., Haile, M., Govers, G., and Moeyersons, J.: Effectiveness of stone bunds in controlling soil erosion on cropland in the Tigray highlands, Northern Ethiopia, Soil Use. Manage., 21, 287-297, 2005.

Global Land Cover Characterization (GLCC): http://edcsns17.cr.usgs.gov/glcc/glcc.html, access: 20 September 2007.

Green, W. H., and Ampt, C. A.: Studies on soil physics: I. Flow of air and water through soils, J. Agr. Sci., 4, 1–24, 1911.

Gupta, H., Sorooshian, S., and Yapo, P.: Status of automatic calibration for hydrologic models: Comparison with multilevel expert calibration, J. Hydrol. Eng., 4, 135-143, 1999.

Haregeweyn, N., and Yohannes, F.: Testing and evaluation of the agricultural non-point source pollution model (AGNPS) on Augucho catchment, western Hararghe, Ethiopia, Agr. Ecosyst. Environ., 99, 201-212, 2003.

Hargreaves, G., Hargreaves, G., and Riley, J.: Agricultural benefits for Senegal River basin, J. Irrig. Drain. E-ASCE, 111, 113-124, 1985.

Hengsdijk, H., Meijerink, G., and Mosugu, M.: Modeling the effect of three soil and water conservation practices in Tigray, Ethiopia, Agr. Ecosyst. Environ., 105, 29-40, 2005.

Herweg, K., and Ludi, E.: The performance of selected soil and water conservation measures--case studies from Ethiopia and Eritrea, Catena, 36, 99-114, 1999.

Hurni, H.: Soil erosion and soil formation in agricultural ecosystems: Ethiopia and Northern Thailand, Mt. Res. Dev., 3, 131-142, 1983.

Hurni, H.: Erosion - productivity - conservation systems in Ethiopia, in: Proceedings of the 4th International Conference on Soil Conservation, Maracay, Venezuela, 654-674, 1985.

Hurni, H.: Land degradation, famine, and land resource scenarios in Ethiopia, in: World Soil Erosion and Conservation, edited by: Pimentel, D., Cambridge University Press, Cambridge, UK, 27–61, 1993.

Hole-filled SRTM for the globe Version 4: http://srtm.csi.cgiar.org, access: 10 December 2009, 2008.

Kuichling, E.: The relation between the rainfall and the discharge of sewers in populous district, Trans. Am. Soc. Civ. Eng., 20, 37-40, 1989.

Merritt, W. S., Letcher, R. A., and Jakeman, A. J.: A review of erosion and sediment transport models, Environ. Modell. Softw., 18, 761-799, 2003.

Mohammed, H., Yohannes, F., and Zeleke, G.: Validation of agricultural non-point source (AGNPS) pollution model in Kori watershed, South Wollo, Ethiopia, Int. J. Appl. Earth. Obs., 6, 97-109, 2004.

Monteith, J. L.: Evaporation and environment, Symp. Soc. Exp. Biol., 19 205-234, 1965.

Moriasi, D. N., Arnold, J. G., Van Liew, M. W., Bingner, R. L., Harmel, R. D., and Veith, T. L.: Model evaluation guidelines for systematic quantification of accuracy in watershed simulations, T. ASABE, 50, 885-900, 2007.

Nash, J. E., and Sutcliffe, J. V.: River flow forecasting through conceptual models part I--A discussion of principles, J. Hydrol. , 10, 282-290, 1970.

NBCBN: Survey of literature and data inventory in watershed erosion and sediment transport, Nile Basin Capacity Building Network, Cairo, 2005.

Neitsch, S. L., Arnold, J. G., Kiniry, J., and Williams, J. R.: Soil and water assessment tool theoretical documentation (Version 2005), USDA Agricultural Research Service and Texas A&M Blackland Research Center, Temple, Texas, 2005.

Nyssen, J., Haregeweyn , N., Descheemaeker, K., Gebremichael, D., Vancampenhout, K., Poesen, J., Haile, M., Moeyersons, J., Buytaert, W., Naudts, J., Deckers, J., and Govers, G.: Modelling the effect of soil and water conservation practices in Tigray, Ethiopia (Agric. Ecosyst. Environ. 105 (2005) 29–40), Agric. Ecosyst. Environ., 114, 407–411, 2005.

Priestley, C., and Taylor, R.: On the assessment of surface heat flux and evaporation using large-scale parameters, Mon. Weather Rev., 100, 81-92, 1972.

Santhi, C., Srinivasan, R., Arnold, J., and Williams, J.: A modeling approach to evaluate the impacts of water quality management plans implemented in a watershed in Texas, Environ. Modell. Softw., 21, 1141-1157, 2005.

Setegn, S., Dargahi, B., Srinivasan, R., and Melesse, A.: Modeling of Sediment Yield From Anjeni-Gauged Watershed, Ethiopia Using SWAT Model, J. Am. Water Resour. As., 46, 514-526, DOI: 10.1111/j.1752-1688.2010.00431.x, 2010.

Shahin, M.: An overview of reservoir sedimentation in some African river basins, in: Proceedings of Sediment Problems: Strategies for Monitoring, Prediction and Control, Yokohama, July 1993, LAHS Publ. no. 217, 93-100, 1993.

Steenhuis, T., Collick, A., Easton, Z., Leggesse, E., Bayabil, H., White, E., Awulachew, S., Adgo, E., and Ahmed, A.: Predicting discharge and sediment for the Abay (Blue Nile) with a simple model, Hydrol. Process., 23, 3728-3737, 2009.

Sutcliffe, J., and Parks, Y.: The hydrology of the Nile, IAHS Special Publication no. 5, International Association of Hydrological Sciences, Wallingford, UK, 1999.

Tamene, L., Park, S., Dikau, R., and Vlek, P.: Analysis of factors determining sediment yield variability in the highlands of northern Ethiopia, Geomorphology, 76, 76-91, 2006.

U.S. Department of Agriculture – Soil Conservation Service (USDA-SCS): Urban Hydrology for Small Watersheds, USDA, Washington, DC, 1986.

U.S. Department of Agriculture – Soil Conservation Service (USDA-SCS): National Engineering Handbook, Section IV, Hydrology, 4-102pp., 1972.

Vaché, K., Eilers, J., and Santelmann, M.: Water quality modeling of alternative agricultural scenarios in the us corn belt, J. AM. WATER RESOUR. AS., 38, 773-787, 2002.

Van Griensven, A., Meixner, T., Grunwald, S., Bishop, T., Diluzio, M., and Srinivasan, R.: A global sensitivity analysis tool for the parameters of multi-variable catchment models, J. Hydrol., 324, 10-23, 2006.

Verstraeten, G., Poesen, J., Gillijns, K., and Govers, G.: The use of riparian vegetated filter strips to reduce river sediment loads: an overestimated control measure?, HYDROL. PROCESS., 20, 4259-4267, 2006.

Williams, J.: SPNM, a model for predicting sediment, phosphorus, and nitrogen yields from agricultural basins, J. Am. Water. Resour. As., 16, 843-848, 1980.

Williams, J., and Berndt, H.: Sediment yield prediction based on watershed hydrology, T. ASAE 20, 1100-1104, 1977.

Williams, J. R.: Flood routing with variable travel time or variable storage coefficients, T. ASAE, 12, 100-103, 1969.

World Bank: Africa Development Indicators 2006, The International Bank for Reconstruction and Development/ World Bank, Washington, D.C., 2006.

Winchell, M., Srinivasan, R., Di Luzio, M., and Arnold, J. G.: ArcSWAT interface for SWAT2005 User's guide, USDA Agricultural Research Service and Texas A&M Blackland Research Center, Temple, Texas, 2007.

Zeleke, G.: Landscape dynamics and soil erosion process modelling in the north-western Ethiopian highlands, in: African Studies Series A, Geographica Bernensia, Berne, 2000.

Zeleke, G., and Hurni, H.: Implications of land use and land cover dynamics for mountain resource degradation in the northwestern Ethiopian highlands, Mt. Res. Dev., 21, 184-191, 2001.

Table 1. Spatial model input data for the Upper Blue Nile.

Data type	Description	Resolution	Source
Topography map	Digital Elevation Map (DEM)	90 m	SRTM
Land use map	Land use classifications	1 km	GLCC
Soils map	Soil types	10 km	FAO
Weather	Daily precipitation and minimum and maximum temperature	17 stations	Ethiopian Ministry of Water Resources

Table 2. Land use/ Land cover types and area coverage in the Upper Blue Nile.

Landuse	Description	Area (%)
Dryland Cropland	Land used for agriculture crop	17
Cropland	Land area covered with mixture of croplands, shrublands, and grasslands	5.8
Grassland	Land covered by naturally occurring grass	2.5
Shrubland	Lands characterized by xerophytic vegetative types	1.1
Savanna	Lands with herbaceous and other understory systems height exceeds 2 m height	68.8
Deciduous Broadleaf Forest	Land dominated by deciduous broadleaf trees	0.02
Evergreen Broadleaf Forest	Land dominated by evergreen broadleaf trees	1.6
Mixed Forest	Land covered by both deciduous and evergreen trees	0.7
Water Body	Area within the landmass covered by water	2.2
Barren	Land with exposed rocks and limited ability to support life	0.4
Residential Medium Density	Land area covered by structures such as town	0.2

Table 3. Scenarios description and SWAT parameters used to represent BMPs.

Scenarios	Description	SWAT parameter used			
		Parameter name (input file)		Calibration value	Modified value
Scenario-0	baseline	-		*	*
Scenario-1	buffer strip	FILTERW (.hru)**		0	1 (m)
Scenario-2	stone-bund	SLSUBBSN (.hru)	0-10% slope	61 (m)	10 (m)
			10-20% slope	24 (m)	10 (m)
			>20% slope	9.1 m	9.1 (m)
		CN2 (.mgt)		81	59
		USLE_P (.mgt)		0.53	0.32
Scenario-3	reforestation	-		*	*

*Assigned by SWAT model.

** The extensions, .hru and .mgt are input files, where parameter value was edited.

Table 4. SWAT sensitive parameters and fitted values.

Variable	Parameter name	Description	Fitted parameter value
Flow	r__CN2.mgt*	Curve number	-0.02
	v__ALPHA_BF.gw**	Baseflow alpha factor	0.29
	v__GW_DELAY.gw	Groundwater delay time	215.59
	v__GWQMN.gw	Threshold water depth in the shallow aquifer	-596.16
	v__GW_REVAP.gw	Ground water revap co-efficient	-0.46
	v__REVAPMN.gw	Threshold water depth in the shallow aquifer for revap	233.24
	v__ESCO.hru	Soil evaporation compensation factor	0.58
	v__RCHRG_DP.gw	Recharge to deep aquifer	1.07
	v__CH_K2.rte	Channel effective hydraulic conductivity	4.22
	r__SOL_AWC.sol***	Available water capacity	0.54
	r__SOL_K.sol	Saturated hydraulic conductivity	0.00
	r__SURLAG.bsn	Surface runoff lag time	33.6
	r__SLSUBBSN.hru	Average slope length	90.68
	v__CH_N2.rte	Manning's 'n' value for main channel	0.16
Sediment	v__USLE_C {Dryland}	USLE land cover factor	0.29
	v__USLE_C{Cropland}	Soil erosion land cover factor	0.03
	v__USLE_C{Savanna}	USLE land cover factor	0.17
	v__USLE_C{Grassland}	USLE land cover factor	0.35
	v__USLE_C{Shurbland}	USLE land cover factor	0.36
	v__SPCON.bsn	Linear re-entrainment parameter for channel sediment routing	0.01
	v__SPEXP.bsn	Exponent of re-entrainment parameter for channel sediment routing	1.20
	r__USLE_P.mgt	Universal soil loss equation support practice factor	0.53
	v__Ch_COV.rte	Channel cover factor	0.71
	v__Ch_Erod.rte	Channel erodibility factor	0.63
	v__PSP.bsn	Sediment routing factor in main channel	0.12

* The extension (e.g., .mgt) refers to the SWAT input file where the parameter occurs.

** The qualifier (v__) refers to the substitution of a parameter by a value from the given range.

*** The qualifier (r__) refers to relative change in the parameter where the value from the SWAT database is multiplied by 1 plus a factor in the given range.

Table 5. Percent of land paced in BMPs and their effectiveness.

Subbasin	Agricultural HRUs area (%)	Filter strips effectiveness (%)	Stone bunds reduction (%)	Reforestation area (%)	Reforestation effectiveness (%)
1	2	58	62	0.4	77
2	28	65	42	8	48
3	27	29	10	11	46
4	4	58	57	1	69
5	8	61	63	8	72
6	10	68	69	17	74
7	18	43	48	8	69
8	32	29	9	10	46
9	30	49	33	4	55
10	13	50	45	12	56
11	12	50	43	17	63
12	18	67	62	28	62
13	13	54	50	6	60
14	13	47	43	2	64
15	29	60	43	7	50

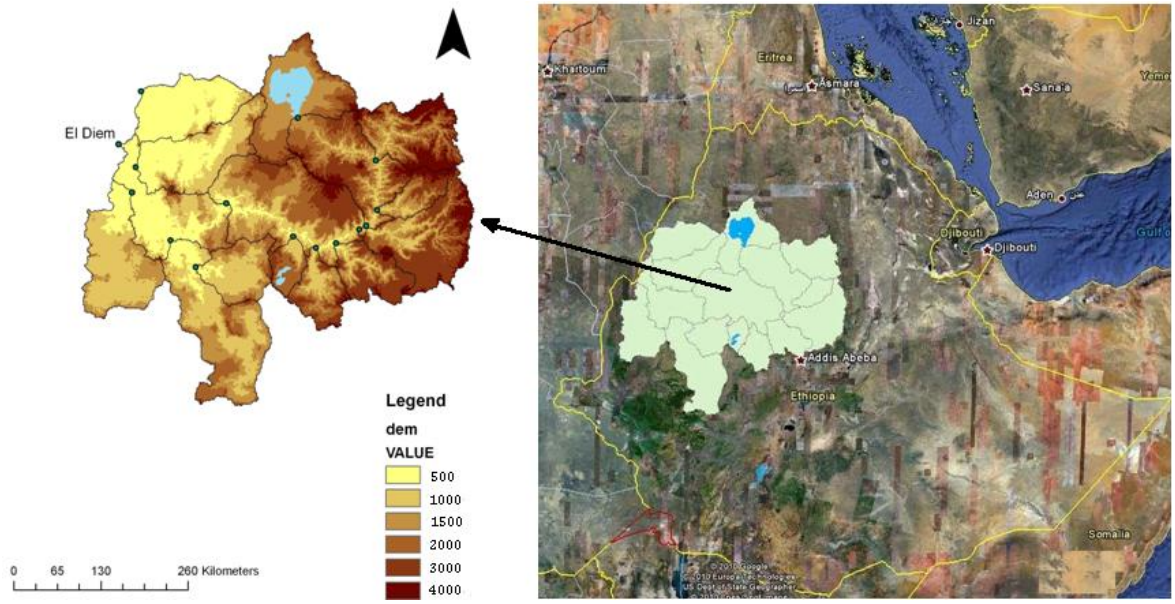

Figure 1. Location map of Upper Blue Nile.

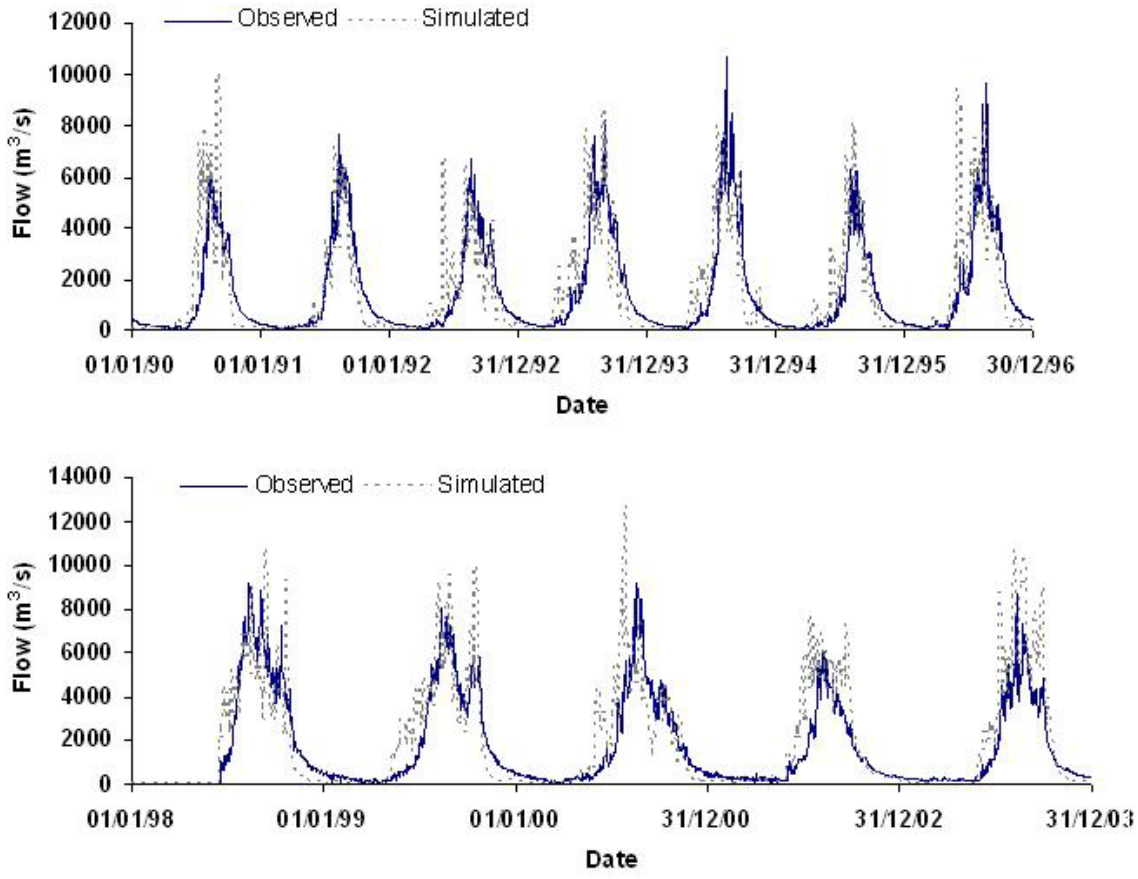

Figure 2. Observed and simulated daily flow hydrographs at El Diem station, calibration (top) and validation (bottom).

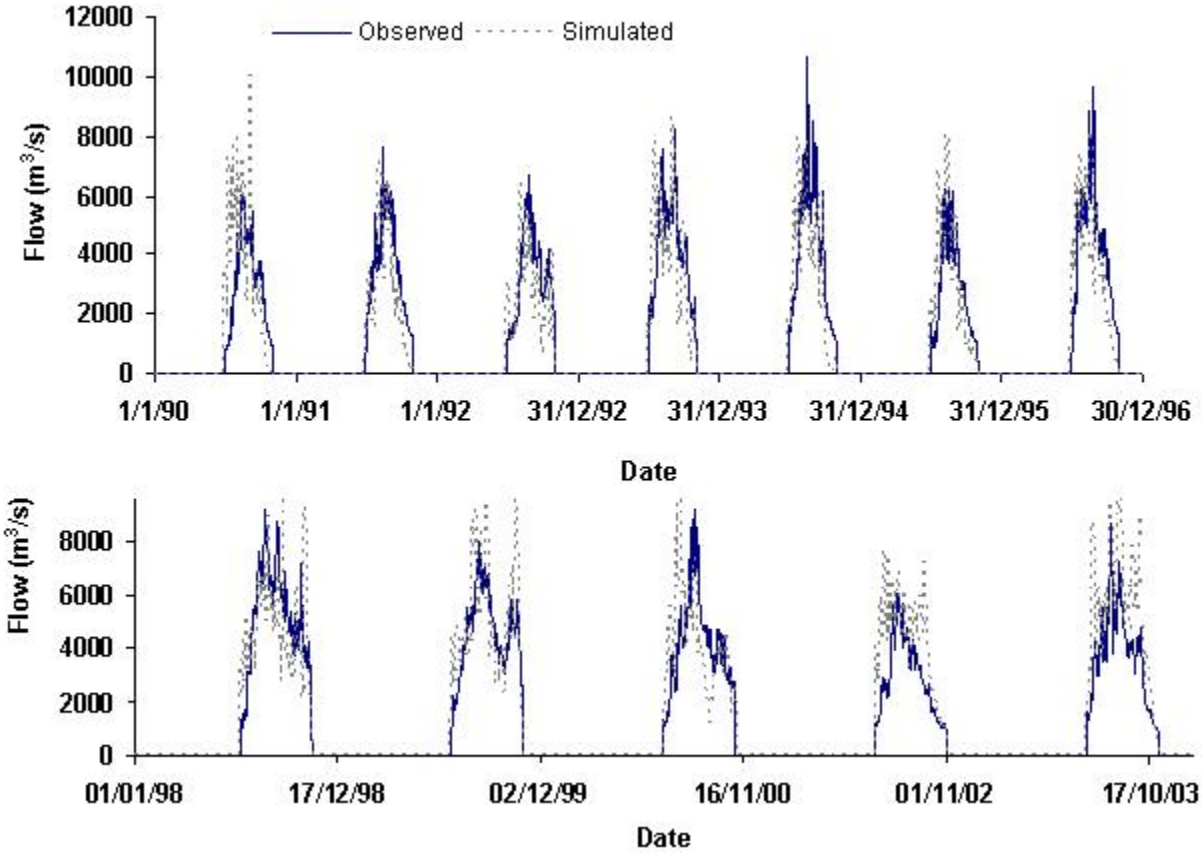

1 Fig. 3. Observed and simulated daily wet-season flow hydrograph at El Diem station, calibration
2 (top) and validation (bottom).

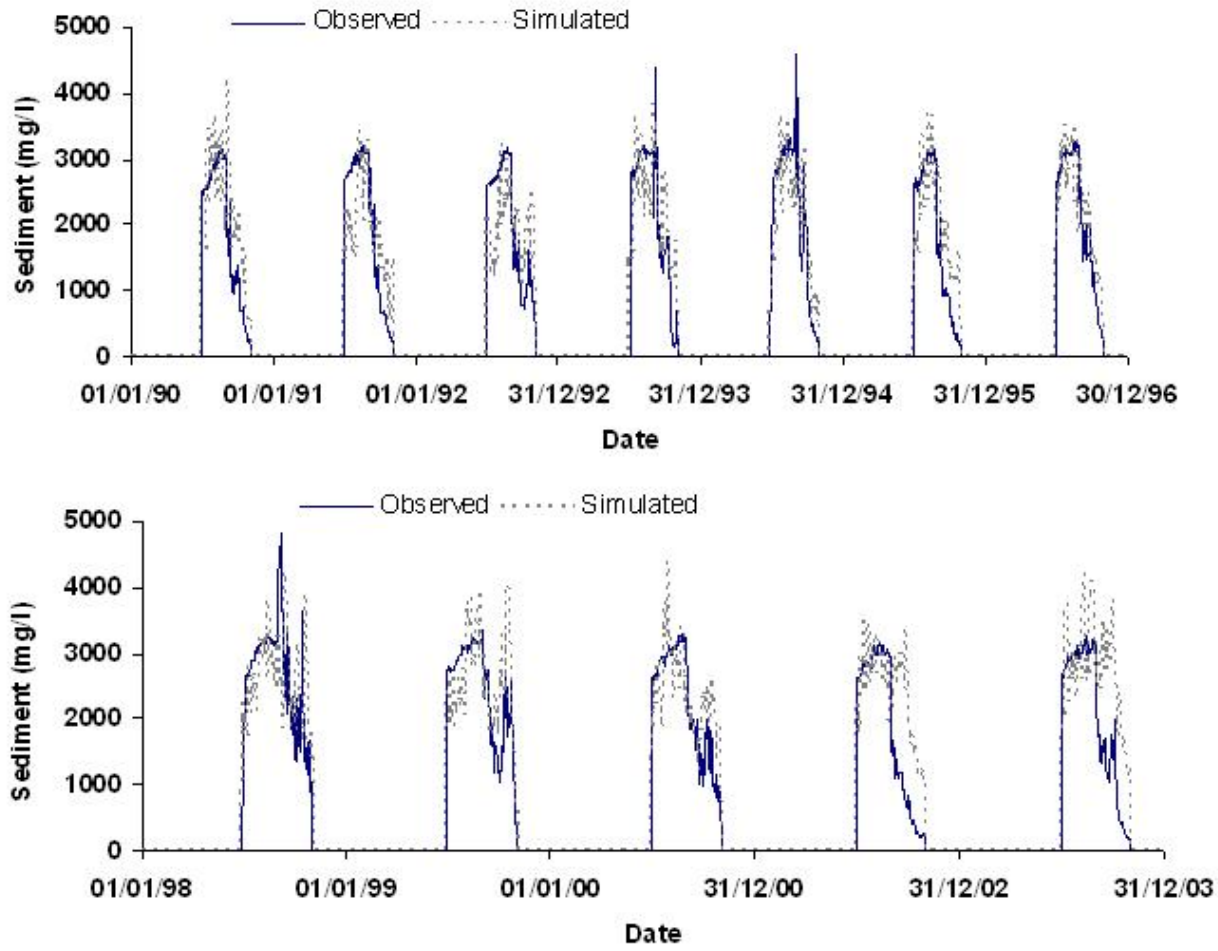

Fig. 4. Observed and simulated daily sediment concentration at El Diem gauging station, calibration (top) and validation (bottom).

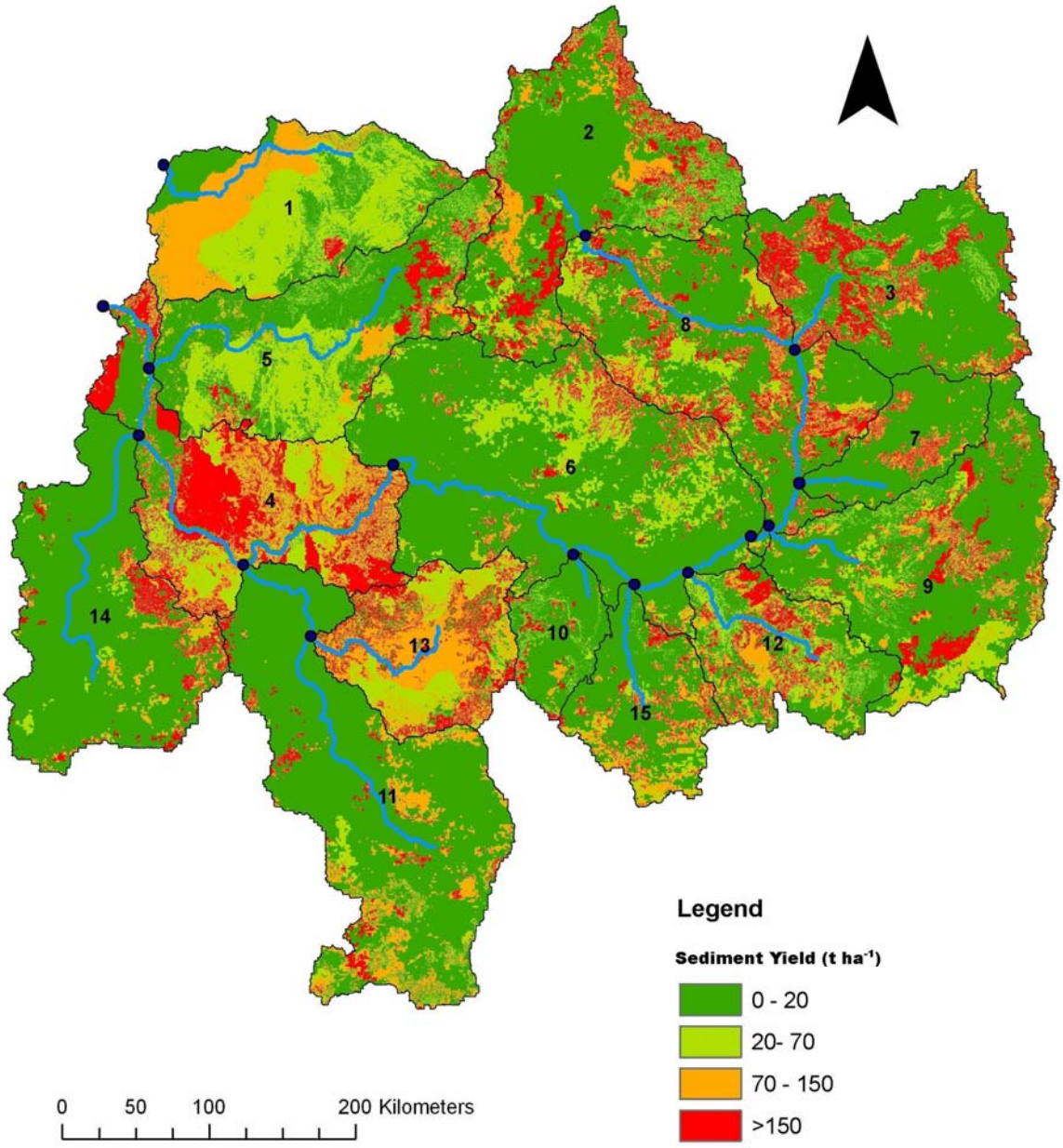

Fig. 5. Relative erosion prone area for existing condition in the Upper Blue Nile.

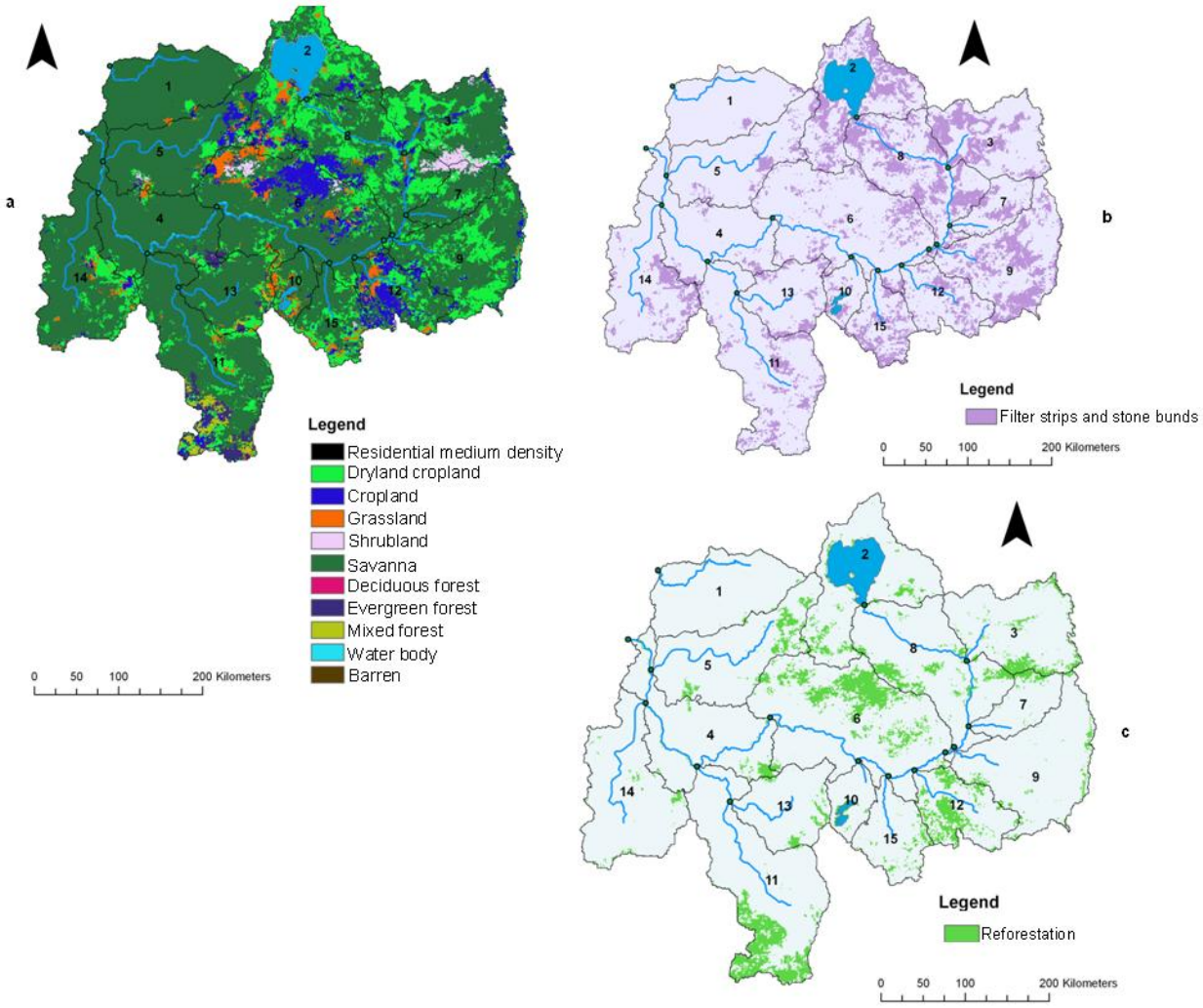

1 Fig. 6. Landuse (a), filter strips and stone bunds (b) and reforestation (c) maps of the Upper Blue
2 Nile.

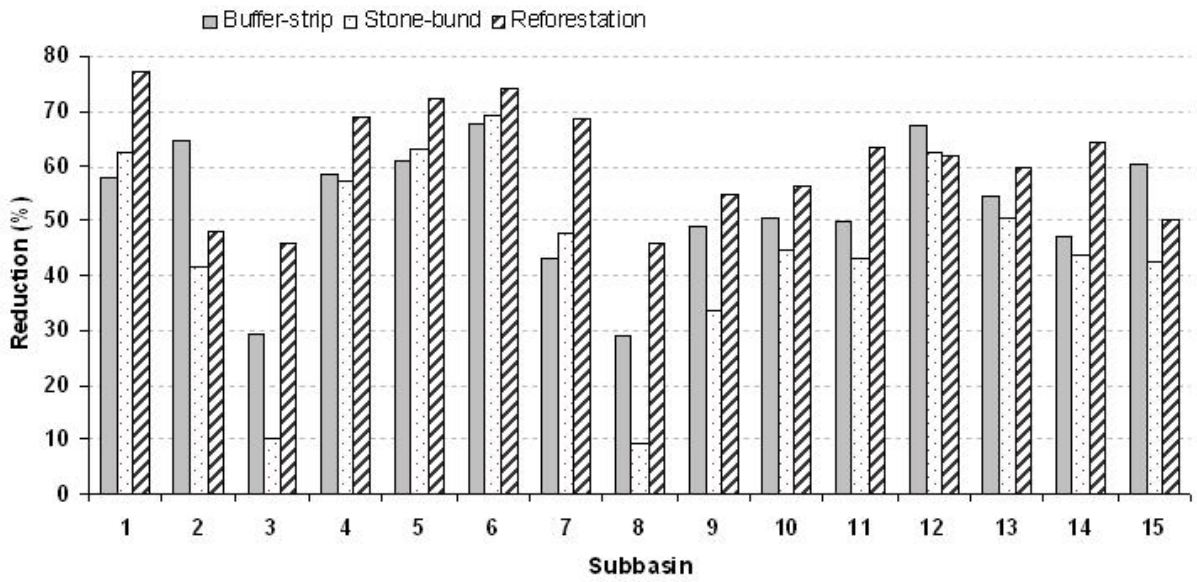

Figure 7. Percent reductions in sediment yield due to BMPs at subbasins level of the Upper Blue Nile basin (the basin outlet is located in the subbasin-4).